Biocatalysis and Agricultural Biotechnology 18 (2019) 101024

Contents lists available at ScienceDirect

Biocatalysis and Agricultural Biotechnology

journal homepage: www.elsevier.com/locate/bab

Antimitotic and DNA-binding potential of biosynthesized ZnO-NPs from leaf extract of *Justicia wynaadensis* (Nees) Heyne - A medicinal herb

N.K. Hemanth Kumar[a], J. Devabrath Andia[a], S. Manjunatha[b], M. Murali[b], K.N. Amruthesh[b], Shobha Jagannath[a,*]

[a] Environmental Biology and Ecotoxicology Laboratory, Department of Studies in Botany, University of Mysore, Manasagangotri, Mysuru, 570 006, Karnataka, India
[b] Applied Plant Pathology Laboratory, Department of Studies in Botany, University of Mysore, Manasagangotri, Mysuru, 570 006, Karnataka, India

ARTICLE INFO

Keywords:
Allium cepa
CT-DNA
Nanoparticles
Mitotic index
Chromosomal abnormality

ABSTRACT

Zinc oxide nanoparticles (ZnO-NPs) synthesized through biological method has gained significant importance due to its wide range of applications. In the current study, hexagonal wurtzite shaped nanoparticles were bio-synthesized using the aqueous leaf extract of *Justicia* wynaadensis for the first time. The bio-synthesized ZnO-NPs showed an absorption peak at 329 nm which is the characteristic feature of ZnO-NPs. The biosynthesized nanoparticles were of high purity with an average size of ~39 nm. The SEM images further confirmed the same with agglomeration of nanoparticles. The Fourier Transform Infrared Spectroscopy (FT-IR) confirmed that the metabolites of plant extract were capped during the bio-synthesis process of nanoparticles. The results of antimitotic activity confirmed that, the biosynthesized ZnO-NPs effectively inhibits the cell division from 100 μg mL^{-1} to 500 μg mL^{-1}. The interaction between CT-DNA and biosynthesized ZnO-NPs showed a hyperchromic shift in absorbance thereby indicating that the DNA structure was changed after addition of ZnO-NPs through intercalate mode. The results validate that the biosynthesized ZnO-NPs form *Justicia wynaadensis* possess biological activities.

1. Introduction

Nanotechnology is one of the emerging fields' with broad application in the field of science and technology. A recent advance to manufacture new materials of any size and shape at a highly ordered condition has paved the way for the development of new biocidal agents (Devi and Gayathri, 2014). Even though conventional methods use less time for synthesizing nanoparticles, they contribute to environmental toxicity because they require toxic chemicals as capping agents (Mahendra et al., 2017). Hence, a lot of attention has been diverted to biosynthesis of metal nanoparticles using biotic sources as reducing and stabilizing agents due to their eco-friendly and non-toxic nature (Murali et al., 2017).

Metal oxides with nanostructure have attracted considerable interest in many areas of technology. Among metal oxide nanoparticles like copper (Harne et al., 2012), titanium (Sundrarajan and Gowri, 2011) and gold (Smitha et al., 2009), ZnO has not received much attention in the recent past (Dobrucka and Długaszewska, 2016). Zinc oxide (ZnO) is a unique and a key inorganic material and has attracted extensive research because of its characteristic features and novel applications in broad areas of science and technology. ZnO nanoparticles (ZnO-NPs) hold unique properties like semiconducting, pyroelectric, piezoelectric, catalysis and optoelectronics. Apart from these physico-chemical properties, these particles are also known for their biological applications and also possess non-toxic nature to human cells (Anbuvannan et al., 2015; Mahendra et al., 2017).

Among the biological materials used for the synthesis of nanoparticles, plants seem to be the best candidates and they are suitable for the large-scale biosynthesis. Nanoparticles synthesized using plant extracts are more stable and vary in size and shape compared to chemically synthesized nanoparticles as the metabolites present in the plants acts as capping and stabilizing agents during the biosynthesis process (Gunalan et al., 2012; Dobrucka and Długaszewska, 2016). It has observed that zinc acts as an essential mineral that is integral to many enzymes and transcription factors that regulate cellular functions like oxidative stress, DNA replication, DNA damage repair, cell cycle progression and apoptosis (Sabir et al., 2014). Onion (*Allium cepa*) is considered to be a good bioindicator for genotoxicity and clastogenicity studies as authenticated by the environmental protection agencies such as the United Nations Environmental Programme (UNEP) and the

* Corresponding author. Environmental Biology and Ecotoxicology Laboratory, Department of Studies in Botany, University of Mysore, Manasagangotri, Mysore, 570006, Karnataka, India.
E-mail addresses: hemanthbot@gmail.com (N.K. Hemanth Kumar), shobhajags25@gmail.com (S. Jagannath).

https://doi.org/10.1016/j.bcab.2019.101024
Received 21 September 2018; Received in revised form 18 January 2019; Accepted 31 January 2019
Available online 01 February 2019
1878-8181/

United States Environmental Protection Agency (USEPA) (Thenmozhi et al., 2011). *Allium cepa* root meristematic cells have been used extensively in the screening of drugs including nanoparticles as the root tip assay provides another better way of detecting the antimitotic potential (Thenmozhi et al., 2011; Mahendra et al., 2017).

Justicia wynaadensis (Nees) Heyne is an important medicinal plant distributed in the Western Ghats of India (Patil et al., 2015). The plant juice (from stem and leaves) is generally consumed as a sweet dish and possess unique flavor due to different medicinal principals that improve human health. The plant is used against the treatment of asthma, inflammatory and rheumatic swellings (Medapa et al., 2011). Due to vast ethnomedicinal importance of *J. wynaadensis*, the current investigation has been undertaken to evaluate the antimitotic and DNA-binding properties of bio-synthesized ZnO-NPs from *J. wynaadensis*. Presently, there are no reports on the biosynthesis of any of the metal nanoparticles from *J. wynaadensis* and the present study is the first report on the biosynthesis of ZnO-NPs.

2. Materials and methods

2.1. Collection of plant material

The healthy leaves of *Justicia wynaadensis* were collected from Madikeri, Western Ghats, Karnataka, India. The plant was identified using Flora of Presidency of Madras (Gamble, 1935) and authenticated by Prof. M.S. Sudarshana (Taxonomist), Department of Studies in Botany, University of Mysore, Mysuru.

2.2. Bio-synthesis of zinc oxide nanoparticles (ZnO-NPs) from Justicia wynaadensis

The biosynthesis of ZnO-NPs from aqueous extract of *Justicia wynaadensis* was carried out following the method of Murali et al. (2017). Twenty five grams of fresh leaf material was extracted with 100 mL of sterile distilled water and filtered. About 50 mL of filtrate was boiled to 60 °C using magnetic stirrer and when the temperature reached 60 °C about 5 g of zinc nitrate hexahydrate (Fine-Chem Ltd., India) was added and allowed until the solution becomes a paste. The obtained material was transfer to the ceramic crucible and kept in a furnace at 350 °C for 3 h. The final obtained powdered product (ZnO-NPs) was stored and used for further studies. Preliminary phytochemical analysis of the plant extract was carried out using the method described by Harborne (1973) and Trease and Evans (1987) and GC-MS analysis of the extract was also carried out using Shimadzu GC-MS (Model QP2010S, Japan).

2.3. Characterization of biosynthesized ZnO-NPs

2.3.1. UV-Vis spectroscopy

The bio-reduction of ZnO was measured using UV–Vis Spectrophotometer. The spectral analysis of ZnO-NPs was carried out by measuring the optical density (OD) using Beckman Coulter, (DU739, Germany) scanning UV–Vis Spectrophotometer operated at a resolution of 1 nm between 200 and 800 nm.

2.3.2. X-ray powder diffraction (XRD) analysis

X-Ray diffraction (XRD) patterns of bio-synthesized ZnO-NPs was performed on a Rigaku Desktop Miniflex II X-Ray powder diffractometer with Cu kα radiation, (λ = 1.5406 Å) as the energy source and the diffraction intensities were recorded between 20 and 80° 2θ angles. The size of bio-synthesized particles was calculated by Scherrer's formula.

$$\Phi = \frac{K\lambda}{\beta\cos\theta}$$

where: Φ – the crystal size; λ – the wavelength of the X-ray radiation (λ = 0.15406 nm) for CuKα, K – usually taken as 0.89; β – the line width at the half-maximum height.

2.3.3. Scanning Electron microscopy (SEM) and energy dispersive spectroscopy (EDS) analysis

The bio-synthesized ZnO-NPs were placed on the carbon-coated copper grid in a tiny amount and allowed to air dry. The images were captured using scanning SEM (HITACHI- S-3400 N, Japan) with 15 kV acceleration voltages to examine their morphology. The Energy Dispersive Spectroscopy (EDS) analysis was carried out using HITACHI Noran System 7 (USA) attached to SEM for the detection of metals in the biosynthesized ZnO-NPs. The study revealed the qualitative and quantitative amounts of metal elements present in the biosynthesized ZnO-NPs.

2.3.4. Fourier Transform Infra-Red (FT-IR) spectroscopy

Bio-synthesized ZnO-NPs were evaluated for their binding properties by FT-IR analysis. The FT-IR analysis of the plant extract and biosynthesized ZnO-NPs were carried out on Perkin Elmer Spectrum 1000 in attenuated total reflection mode using the spectral range of 4000 to 400 cm^{-1} at a resolution of 4 cm^{-1}.

2.4. Antimitotic potential of biosynthesized ZnO-NPs

The antimitotic potential of bio-synthesized ZnO-NPs on healthy roots tips of *Allium cepa* L. were carried out following the method of Levan (1938). Old roots of onion bulbs were scraped away without affecting the root primordia and allowed to sprout on a vial containing sterile distilled water (SDW). When the roots were about 2–3 cm long, the roots of the onion bulbs were exposed to different concentrations of ZnO-NPs (100, 200, 300, 400 and 500 μg mL^{-1}) for 24 h at room temperature. Methotrexate and SDW served as positive and negative control, respectively. After incubation, the root tips of each bulb were carefully excised and transferd into Carnoy's solution II for about 24 h. After incubation, the root tips were transferred to 70% ethanol. The fixed root tips were squashed following the method of Fiskesjo (1985). The slides were observed to record the total number of cells, dividing cells and chromosomal aberrations under a microscope. Mitotic index was calculated using the formula

$$\text{Mitotic Index} = \frac{\text{Number of dividing cells}}{\text{Total number of cells}} \times 100$$

2.5. DNA binding potential of biosynthesized ZnO-NPs

The interaction between *Calf thymus* DNA (CT-DNA) and bio-synthesized ZnO-NPs were investigated following the method of Firdhouse and Lalitha (2015). The CT-DNA stock solution [1 mg of CT-DNA in 10 mL Tris-HCl buffer (10 mM, pH 7.4)] gave an absorption value of 1.8 and 1.9 at 260 and 280 nm, respectively indicating the solution is free from protein. The DNA binding potential of ZnO-NPs were carried out by keeping constant DNA concentration (100 μg mL^{-1}) and varying the concentration nanoparticle from 100 to 500 μg mL^{-1}. The mixture was incubated for 30 min and the changes in absorbance spectra (between 200 and 800 nm) were observed.

2.6. Statistical analysis

All the experiments were carried out in three replicates and the data of each experiment was subjected to Analysis of variance (ANOVA) using SPSS Inc. 16.0. Significant effects of the treatments were determined by F values ($p \leq 0.05$). Treatment means was separated by Tukey's HSD.

Table 1
GC-MS analysis of *J. wayanadensis* leaf aqueous extract.

Peak	R. Time	Area	Area (%)	Height	Height (%)	Name	Base (m/z)
1	17.761	38812	22.22	8462	31.56	2H-1-BENZOPYRAN-2-ONE	118.05
2	17.802	91031	52.13	8643	32.24	2-D(1)-4-PHENYLOXAZOLE	90.05
3	18.024	18119	10.38	6190	23.09	1,3,5-TRIOXANE	89.05
4	18.443	8335	4.77	1100	4.10	1,3,4,5-TETRA-O-ACETYL,2,6,7-TRI-O-METHYL-D[1]-HEPTITOL	118.05
5	42.797	18342	10.50	2415	9.01	EPIBROMHYDRIN	57.10
		174639	100.00	26810	100.00		

3. Results and discussion

3.1. Bio-synthesis of zinc oxide nanoparticles (ZnO-NPs) from Justicia wynaadensis

The preliminary phytochemical analysis of the aqueous plant extract showed the presence of alakaloids, phenolic compounds and flavonoids (Suppl. Table 1). The GC-MS analysis carried out revealed the presence of five major peaks which belong to different groups (Table 1). From the GC-MS analysis it was observed that 2-D(1)-4-Phenyloxazole was the major compound and the oxazole group is know to possess many biological properties (Singh et al., 2016). The mechanism of formation of the ZnO-NPs involves the interaction of polymer chains of the *J. wynaadensis* extract resulting in the cross-link between the chains. To understand the possible mechanism of formation of ZnO-NPs with one of the identified compounds from aqueous plant extract (through GC-MS) has been depicted in Fig. 1 by "egg-box" model. The egg box model has been employed by various researchers to identify the possible mechanism of action in the formation of stable nanoparticles through plant extracts during synthesis (Lakshmeesha et al., 2014; Deepthi et al., 2018). Further, the exact mechanism between the contents of any plant extract with metal ions leading to the formation of ZnO-NPS is still needs to be identified.

3.2. Characterization of biosynthesized ZnO-NPs

3.2.1. UV-Vis spectral analysis

UV-Vis spectral analysis was carried out by dispersing bio-synthesized ZnO-NP in distilled water. The spectral data of the present study showed an absorption peak at 329 nm which is characteristic to ZnO (Fig. 2). The results are in confirmation with the previous findings, wherein it was reported that ZnO show absorption peaks between 280 and 400 nm irrespective of their type of synthesis which is correlated to their biological properties (Sharma et al., 2016). Likewise, other researchers have also reported an absorption peak in the range of 280–400 nm of biosynthesized ZnO-NPs (Anbuvannan et al., 2015; Murali et al., 2017).

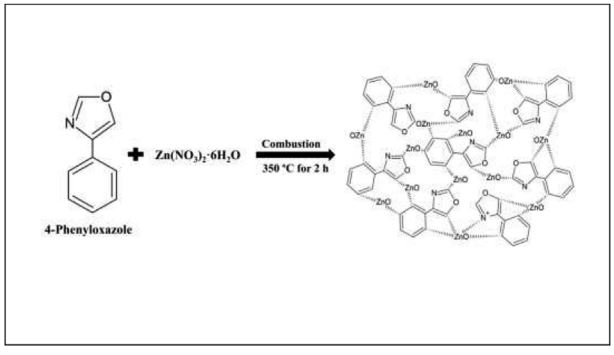

Fig. 1. Egg-box model for trapping metabolite (4-Phenyloxazole) of *J. wynaadensis* aqueous extract for the formation of ZnO-NPs.

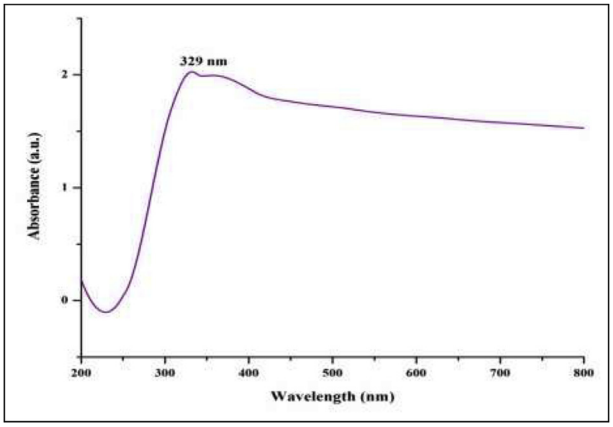

Fig. 2. UV-Vis spectra of biosynthesized ZnO-NPs from *Justicia wynaadensis*.

3.2.2. X-ray powder diffraction (XRD) analysis

The XRD patterns of bio-synthesized ZnO-NPs showed noticeable 2θ peaks at 31.68°, 34.39°, 36.18°, 47.46°, 56.52°, 62.89°, 66.30°, 67.95° and 69.09° which corresponds to correspond to (100), (002), (101), (102) (110), (103), (200), (112) and (201) planes of wurtzite (Fig. 3). Particle size calculated using Scherrer's formula for intense/sharp peaks revealed that the particles were of the average size ~39 nm. The diffraction patterns are indexed to pure hexagonal wurtzite structured ZnO (space group P63mc) with lattice constants and match to JCPDS No. 79–206. The stiff and narrow diffraction peaks of ZnO-NPs confirmed the crystalline structure and indicate the product was without any impurities. Previously, it was reported that the stiff, narrow peaks indicate the purity of the nanoparticles (Mahendra et al., 2017). Accordingly, ZnO nanoparticles biosynthesized using *Trifolium pretense* was also of hexagonal wurtzite shape with 60–70 nm size as calculated through Scherrer's formula (Dobrucka and Długaszewska, 2016).

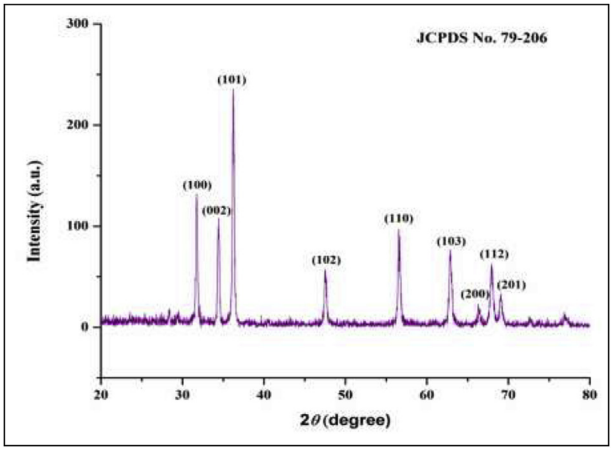

Fig. 3. XRD analysis of biosynthesized ZnO-NPs from *Justicia wynaadensis*.

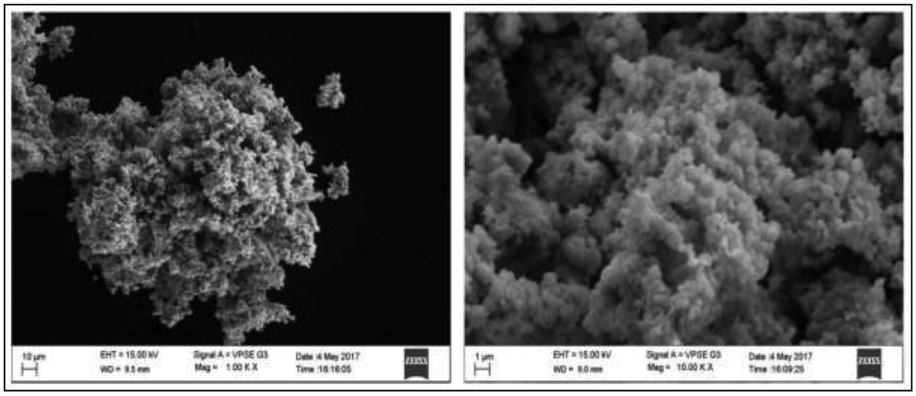

Fig. 4. Scanning Electron microscopic images of biosynthesized ZnO-NPs from *Justicia wynaadensis*.

3.2.3. Scanning Electron microscopy (SEM) and energy dispersive spectroscopy (EDS) analysis

The SEM images showed agglomeration of bio-synthesized ZnO-NPs and hexagonal shape (Fig. 4). The SEM images are in correlation with the findings of XRD analysis. Further, quantitative as well as the qualitative study on ZnO-NPs through EDS revealed a high proportion of Zinc (71.17%) in the synthesized nanoparticles followed by oxygen (23.01%) and carbon (5.82%). The EDS analysis confirmed that the bio-synthesized ZnO-NPs were of high purity and the synthesis process was carried out in accordance (Fig. 5). Accordingly, it has been reported that irrespective of the synthesis process of ZnO-NPs (both bio-synthesized and chemically synthesized), showed a high content of Zn and agglomeration of nanoparticles when analyzed through SEM and EDS (Kumar et al., 2013; Anbuvannan et al., 2015).

3.2.4. Fourier Transform Infra-Red (FT-IR) spectroscopy

The FT-IR analysis of bio-synthesized ZnO-NPs revealed a spectrum band at 2319.78 cm^{-1}, 1457.17 cm^{-1}, 1128.42 cm^{-1} and 557.21 cm^{-1} correspond to aromatic, aliphatic and metal oxide groups. The results affirm that alcohol/phenol and alkyne groups may have capped during the bio-synthesis process. It was also noted that the adsorption peak observed around 3250 cm^{-1} in plant extracts were not found in ZnO-NPs spectral data indicating that the biosynthesized ZnO-NPs were free from moisture (Fig. 6). Likewise, Murali et al. (2017) have observed a peak absorbance in the range of 400–600 cm^{-1} which correspond to Zn−O bonding which were absent in the FT-IR spectra of plant extract. The results are also in concurrence with the findings of Ochieng et al. (2015) where an absorption peak at 510.47 cm^{-1} is attributed to metal-oxide (M-O) vibration band.

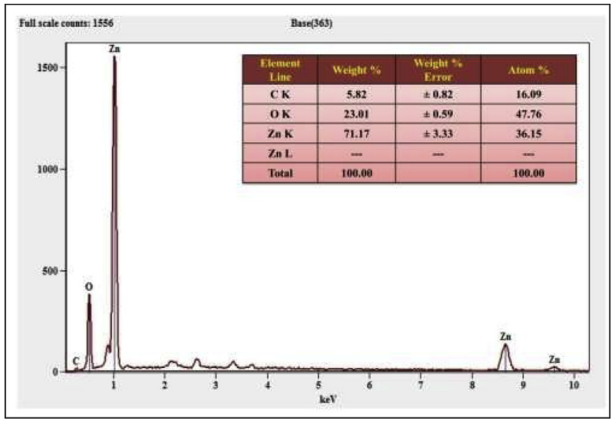

Element Line	Weight %	Weight % Error	Atom %
C K	5.82	± 0.82	16.09
O K	23.01	± 0.59	47.76
Zn K	71.17	± 3.33	36.15
Zn L	---	---	---
Total	100.00		100.00

Fig. 5. Energy Dispersive Spectroscopy analysis of biosynthesized ZnO-NPs from *Justicia wynaadensis*.

3.3. Antimitotic potential of biosynthesized ZnO-NPs

Allium cepa has been used to evaluate the antimitotic properties of bio-synthesized ZnO-NPs and the results are depicted in Fig. 7. The total number of cells and dividing cells decreased in root tips of onion which were treated with ZnO-NPs with increase in concentration compared to control. The mitotic index decreased from 35.16% to 19% and correspondingly, the mitotic inhibition percentage improved from 54.33% to 75.31% with an increase in the concentration of ZnO-NPs. The positive control [methotrexate (500 μg mL^{-1})] offered 17.87% and 77.1% mitotic index and inhibition, respectively. The results demonstrate that upon treatment with ZnO-NPs, there is an increase in chromosomal abnormalities leading to the reduction in dividing cells (Fig. 8). The results are in agreement with the results of Mahendra et al. (2017), wherein ZnO-NPs synthesized using the leaf extract of *C. religiosum* offered inhibition in cell division when the onion root tips were exposed to nanoparticle treatment. The results are also in corroboration with the antimitotic potential of Se-doped ZnO nanoparticles, where Sowbhagya and Ananda (2014) reported a maximum mitotic index of 33.70% in onion root tips.

3.4. DNA binding potential of biosynthesized ZnO-NPs

The interaction between ZnO-NPs and CT-DNA was carried out by monitoring the changes in absorption with UV-Vis spectroscopy. The results suggest that the bio-synthesized ZnO-NPs irrespective of the concentration used intercalated into the DNA molecules which was confirmed by the hyperchromic shift in absorbance (Fig. 9). The typical hyperchromic shift in absorption indicates that the DNA structure was changed through intercalate mode after addition of ZnO-NPs. The results corroborate with the findings of Babu et al., (2015) wherein, a shift in absorption above 280 nm was observed upon interaction of CT-DNA with ZnO-NPs. In accordance, Firdhouse and Lalitha (2015) have also reported the binding properties of biosynthesized gold nanoparticles with CT-DNA *in vitro*.

4. Conclusions

The physico-chemical characterization of bio-synthesized ZnO-NPs from *J. wynaadensis* showed high purity, hexagonal wurtzite shape and size within the nanoscale range. The FT-IR studies confirmed that the ZnO-NPs were free from moisture and also evidenced the capping of the metabolites of plant extract during the bio-synthesis process. The results of antimitotic assay reported a reduction in mitotic index in *A. cepa* root tips upon treatment with ZnO-NPs, on the other hand they also possessed DNA binding properties. The results of the study affirm the dual nature, i.e. DNA-binding (in oxidized form) and cytotoxicity (in reduced/dissolved form) thereby warranting *in vivo* studies.

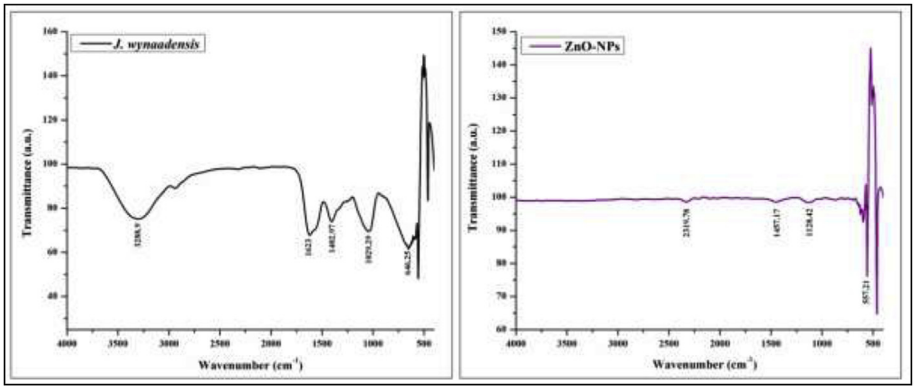

Fig. 6. Fourier Transform Infra-Red (FT-IR) Spectroscopy analysis of biosynthesized ZnO-NPs and *Justicia wynaadensis* aqueous extract. (For interpretation of the references to colour in this figure legend, the reader is referred to the Web version of this article.)

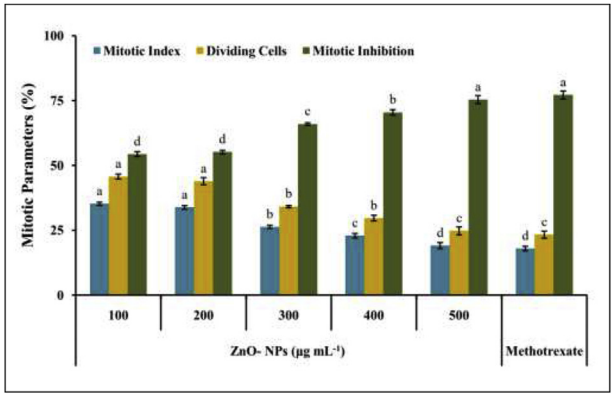

Fig. 7. Effect of biosynthesized ZnO-NPs from *Justicia wynaadensis* on different parameters of antimitotic studies.

Acknowledgments

The authors are thankful to University with Potential for Excellence (UPE) Project Authorities, University of Mysore and Department of Studies in Botany for providing facilities. Murali, M. thank the University Grants Commission (UGC)- New Delhi, India for providing the financial support under UGC Post-Doctoral Fellowship for SC/ST Candidates (No. F/PDFSS-2015-17-KAR-11846). K.N. Amruthesh is grateful to the University of Mysore for awarding Minor Research Project (Univ. Order No. DV6/ 375/ MRP/ 2018-19 Dated 10-2-2018) and for financial assistance.

Appendix A. Supplementary data

Supplementary data to this article can be found online at https://doi.org/10.1016/j.bcab.2019.101024.

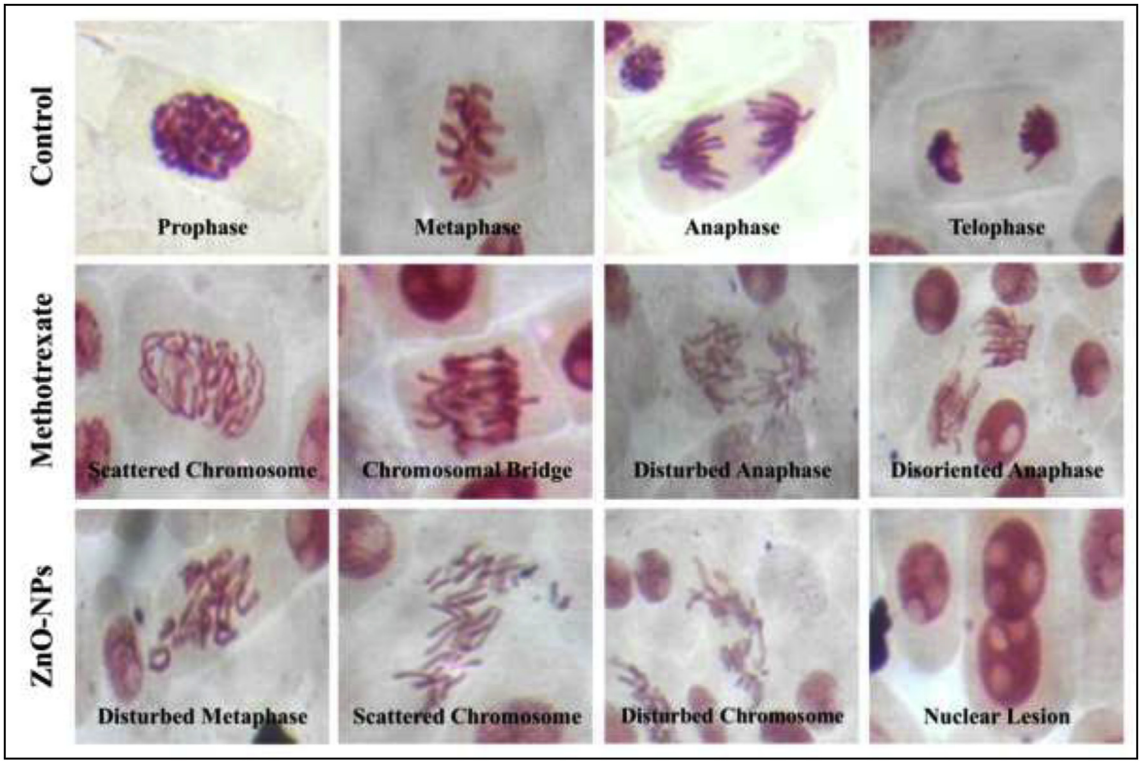

Fig. 8. Compound microscopic analyses show normal mitotic cell division and Chromosomal aberrations induced by Methotrexate and ZnO-NPs in *A. cepa* root meristem cells.

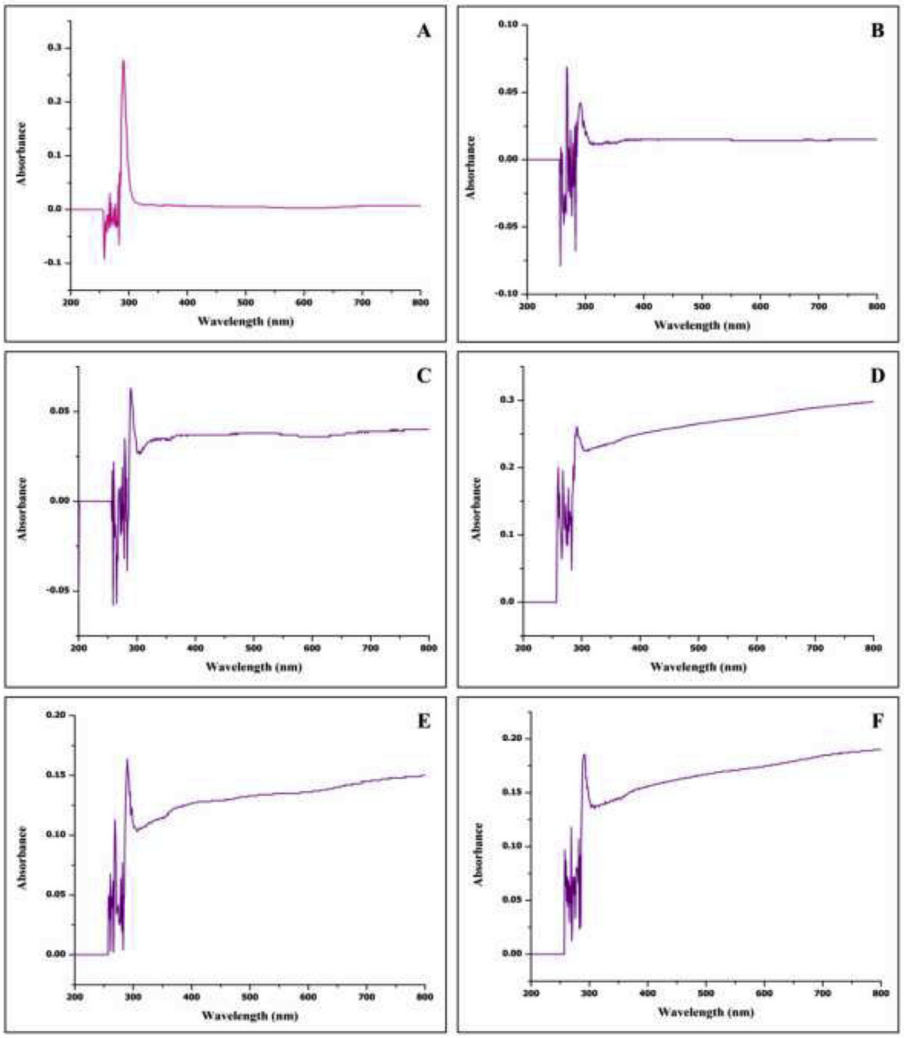

Fig. 9. Absorbance spectra of CT-DNA interaction with ZnO-NPs. A: Only CT-DNA; B: CT-DNA with 100 μg mL^{-1} ZnO-NPs; C: CT-DNA with 200 μg mL^{-1} ZnO-NPs; D: CT-DNA with 300 μg mL^{-1} ZnO-NPs; E: CT-DNA with 400 μg mL^{-1} ZnO-NPs; F: CT-DNA with 500 μg mL^{-1} ZnO-NPs.

References

Anbuvannan, M., Ramesh, M., Viruthagiri, G., Shanmugam, N., Kannadasan, N., 2015. Synthesis, characterization and photocatalytic activity of ZnO nanoparticles prepared by biological method. Spectrochim. Acta Mol. Biomol. Spectrosc. 143, 304–308.

Babu, E.P., Subastri, A., Suyavaran, A., Rao, P.L., Kumar, M.S., Jeevaratnam, K., Thirunavukkarasu, C., 2015. Extracellularly synthesized ZnO nanoparticles interact with DNA and augment gamma radiation induced DNA damage through reactive oxygen species. RSC Adv. 5 (76), 62067–62077.

Deepthi, N.H., Basavaraj, R.B., Sharma, S.C., Revathi, J., Sreenivasa, S., Nagabhushana, H., 2018. Rapid visualization of fingerprints on various surfaces using ZnO super-structures prepared via simple combustion route. J. Sci.: Adv. Mater. Devices 3 (1), 18–28.

Devi, R.S., Gayathri, R., 2014. Green synthesis of zinc oxide nanoparticles by using *Hibiscus rosa-sinensis*. Int. J Curr. Eng. Technol. 4 (4), 2444–2446.

Dobrucka, R., Długaszewska, J., 2016. Biosynthesis and antibacterial activity of ZnO nanoparticles using *Trifolium pratense* flower extract. Saudi J. Biol. Sci. 23 (4), 517–523.

Firdhouse, M.J., Lalitha, P., 2015. Binding properties of biosynthesized gold nanoparticles with calf-thymus DNA *in vitro*. Int. J. Biol. Chem. 9 (4), 188–197.

Fiskesjo, G., 1985. The *Allium* test as a standard in environmental monitoring. Hereditas 102 (1), 99–112.

Gamble, J.S., 1935. In: Fischer, C.E.C. (Ed.), Flora of the Presidency of Madras, Revised Ed.1915.

Gunalan, S., Sivaraj, R., Rajendran, V., 2012. Green synthesized ZnO nanoparticles against bacterial and fungal pathogens. Prog. Nat. Sci. Mater. Int. 22 (6), 693–700.

Harborne, J.B., 1973. Phytochemical Methods. Chapman and Hall Ltd, London, pp. 49–188.

Harne, S., Sharma, A., Dhaygude, M., Joglekar, S., Kodam, K., Hudlikar, M., 2012. Novel route for rapid biosynthesis of copper nanoparticles using aqueous extract of *Calotropis procera* L. latex and their cytotoxicity on tumor cells. Colloids Surfaces B Biointerfaces 95, 284–288.

Kumar, S.S., Venkateswarlu, P., Rao, V.R., Rao, G.N., 2013. Synthesis, characterization and optical properties of zinc oxide nanoparticles. Int. Nano Lett. 3 (1), 30.

Lakshmeesha, T.R., Sateesh, M.K., Prasad, B.D., Sharma, S.C., Kavyashree, D., Chandrasekhar, M., Nagabhushana, H., 2014. Reactivity of crystalline ZnO super-structures against fungi and bacterial pathogens: synthesized using Nerium oleander leaf extract. Cryst. Growth Des. 14 (8), 4068–4079.

Levan, A., 1938. The effect of colchicine on root mitoses in Allium. Hereditas 24 (4), 471–486.

Mahendra, C., Murali, M., Manasa, G., Ponnamma, P., Abhilash, M.R., Lakshmeesha, T.R., Satish, A., Amruthesh, K.N., Sudarshana, M.S., 2017. Antibacterial and antimitotic potential of bio-fabricated zinc oxide nanoparticles of *Cochlospermum religiosum* (L.). Microb. Pathog. 110, 620–629.

Medapa, S., Singh, G.R., Ravikumar, V., 2011. The phytochemical and antioxidant screening of *Justicia wynaadensis*. Afr. J. Plant Sci. 5 (9), 489–492.

Murali, M., Mahendra, C., Rajashekar, N., Sudarshana, M.S., Raveesha, K.A., Amruthesh, K.N., 2017. Antibacterial and antioxidant properties of biosynthesized zinc oxide nanoparticles from *Ceropegia candelabrum* L.– an endemic species. Spectrochim. Acta Mol. Biomol. Spectrosc. 179, 104–109.

Ochieng, P.E., Iwuoha, E., Michira, I., Masikini, M., Ondiek, J., Githira, P., Kamau, G.N., 2015. Green route synthesis and characterization of ZnO nanoparticles using *Spathodea campanulata*. Int. J. BioChem. Phys. 23, 53–61.

Patil, N., Nigudkar, M., Sane, R., Ajitkumar, B.S., Datar, A., 2015. Evaluation of micro-scopic structure of *Justicia wynaadensis* and the stability of its color extracted by using conventional and microwave extraction method. J. Food Sci. Technol. 52 (10), 6455–6464.

Sabir, S., Arshad, M., Chaudhari, S.K., 2014. Zinc oxide nanoparticles for revolutionizing agriculture: synthesis and Applications. Sci. World J., 925494. https://doi.org/10.1155/2014/925494.

Sharma, D., Sabela, M.I., Kanchi, S., Mdluli, P.S., Singh, G., Stenström, T.A., Bisetty, K., 2016. Biosynthesis of ZnO nanoparticles using *Jacaranda mimosifolia* flowers extract: synergistic antibacterial activity and molecular simulated facet specific adsorption

studies. J. Photochem. Photobiol. B Biol. 162, 199–207.
Singh, R.K., Bhatt, A., Kant, R., Chauhan, P.K., 2016. Design and Synthesis of some Novel oxazole derivatives and their biomedicinal efficacy. Chem. Biol. Interface 6 (4), 263–269.
Smitha, S.L., Philip, D., Gopchandran, K.G., 2009. Green synthesis of gold nanoparticles using *Cinnamomum zeylanicum* leaf broth. Spectrochim. Acta Mol. Biomol. Spectrosc. 74 (3), 735–739.
Sowbhagya, Ananda, S., 2014. Synthesis and characterization of se-doped ZnO nanoparticles by electrochemical method: photodegradation kinetics of indigo carmine dye and study of antimicrobial, antimitotic activities of se-doped ZNO nanoparticles. Am. Chem. Sci. J. 4 (5), 616–637.
Sundrarajan, M., Gowri, S., 2011. Green synthesis of titanium dioxide nanoparticles by *Nyctanthes arbor-tristis* leaves extract. Chalcogenide Lett. 8 (8), 447–451.
Thenmozhi, A., Nagalakshmi, A., Mahadeva Rao, U.S., 2011. Study of cytotoxic and antimitotic activities of *Solanum nigrum* by using *Allium cepa* root tip assay and cancer chemo preventive activity using MCF-7-human mammary gland breast adenocarcinoma cell lines. Int. J. Sci. Technol. 1, 26–47.
Trease, G.E., Evans, W.C., 1987. Pharmacognosy. Bailliare Tindall, London.